Temporal Variation of Ecosystem Scale Methane Emission From a Boreal Fen in Relation to Temperature, Water Table Position, and Carbon Dioxide Fluxes

Rinne, Janne

2018-07

Rinne , J , Tuittila , E-S , Peltola , O , Li , X , Raivonen , M , Alekseychik , P , Haapanala , S , Pihlatie , M , Aurela , M , Mammarella , I & Vesala , T 2018 , ' Temporal Variation of Ecosystem Scale Methane Emission From a Boreal Fen in Relation to Temperature, Water Table Position, and Carbon Dioxide Fluxes ' , Global Biogeochemical Cycles , vol. 32 , no. 7 , pp. 1087-1106 . https://doi.org/10.1029/2017GB005747

http://hdl.handle.net/10138/239091
https://doi.org/10.1029/2017GB005747

Global Biogeochemical Cycles

RESEARCH ARTICLE
10.1029/2017GB005747

Key Points:
- Methane emission was insensitive to water table variations observed during decade-long period
- Soil temperature was the dominant driver of methane emission during shorter periods of time (<1 year), while interannual variation was more related to variation in GPP
- Seventy-nine percent of the variability of daily average methane emission is due to seasonal change of drivers, 7.0% is due to interannual variation of drivers, and 5.3% is due to functional change

Supporting Information:
- Supporting Information S1

Correspondence to:
J. Rinne,
janne.rinne@nateko.lu.se

Citation:
Rinne, J., Tuittila, E.-S., Peltola, O., Li, X., Raivonen, M., Alekseychik, P., et al. (2018). Temporal variation of ecosystem scale methane emission from a boreal fen in relation to temperature, water table position, and carbon dioxide fluxes. *Global Biogeochemical Cycles*, *32*, 1087–1106. https://doi.org/10.1029/2017GB005747

Received 20 JUN 2017
Accepted 16 JUN 2018
Accepted article online 27 JUN 2018
Published online 20 JUL 2018

Temporal Variation of Ecosystem Scale Methane Emission From a Boreal Fen in Relation to Temperature, Water Table Position, and Carbon Dioxide Fluxes

Janne Rinne[1], Eeva-Stiina Tuittila[2], Olli Peltola[3], Xuefei Li[3], Maarit Raivonen[3], Pavel Alekseychik[3], Sami Haapanala[3], Mari Pihlatie[3,4], Mika Aurela[5], Ivan Mammarella[3], and Timo Vesala[3,6]

[1]Department of Physical Geography and Ecosystem Science, Lund University, Lund, Sweden, [2]School of Forest Sciences, University of Eastern Finland, Joensuu, Finland, [3]Institute for Atmospheric and Earth System Research/Physics, Faculty of Science, University of Helsinki, Helsinki, Finland, [4]Environmental Soil Science, Department of Agricultural Sciences, Faculty of Agriculture and Forestry, University of Helsinki, Helsinki, Finland, [5]Finnish Meteorological Institute, Helsinki, Finland, [6]Institute for Atmospheric and Earth System Research/Forest Sciences, Faculty of Agriculture and Forestry, University of Helsinki, Helsinki, Finland

Abstract We have analyzed decade-long methane flux data set from a boreal fen, Siikaneva, together with data on environmental parameters and carbon dioxide exchange. The methane flux showed seasonal cycle but no systematic diel cycle. The highest fluxes were observed in July–August with average value of 73 nmol m^{-2} s^{-1}. Wintertime fluxes were small but positive, with January–March average of 6.7 nmol m^{-2} s^{-1}. Daily average methane emission correlated best with peat temperatures at 20–35 cm depths. The second highest correlation was with gross primary production (GPP). The best correspondence between emission algorithm and measured fluxes was found for a variable-slope generalized linear model (r^2 = 0.89) with peat temperature at 35 cm depth and GPP as explanatory variables, slopes varying between years. The homogeneity of slope approach indicated that seasonal variation explained 79% of the sum of squares variation of daily average methane emission, the interannual variation in explanatory factors 7.0%, functional change 5.3%, and random variation 9.1%. Significant correlation between interannual variability of growing season methane emission and that of GPP indicates that on interannual time scales GPP controls methane emission variability, crucially for development of process-based methane emission models. Annual methane emission ranged from 6.0 to 14 gC m^{-2} and was 2.7 ± 0.4% of annual GPP. Over 10-year period methane emission was 18% of net ecosystem exchange as carbon. The weak relation of methane emission to water table position indicates that space-to-time analogy, used to extrapolate spatial chamber data in time, may not be applicable in seasonal time scales.

Plain Language Summary Methane emission from a boreal wetland was measured over one decade. Methane emission shows strong seasonal cycle, with highest emission in late summer and lowest emission during winter. No diel cycle was observed. The methane emission is an important part of the carbon balance of the wetland as 18% of carbon taken up as carbon dioxide was emitted back into atmosphere as methane. The seasonal cycle of the emission was controlled first by peat temperature and second by ecosystem photosynthesis. The interannual variability of methane emission was more related to photosynthesis. A large part of the interannual variability remained unexplained by the measured environmental parameters.

1. Introduction

Methane is the second most important greenhouse gas in contributing to anthropogenic climate change (IPCC, 2013). Its existence and part of origins have been known since observations and experiments by Volta (1777) and its strong infrared absorption properties since experiments by Tyndall (1862). There exist several biogenic and anthropogenic sources of methane into the atmosphere, the most important biogenic one being wetlands (Ciais et al., 2013). In wetlands, the high water-table maintains anaerobic conditions allowing only anaerobic organisms. In northern peat accumulating wetlands, that is, peatlands, organic soils and input of fresh hydrocarbons as root exudates from vegetation provide ideal conditions for methane-producing archaea. The net methane emission from wetland ecosystems is a balance between methane

produced in anaerobic conditions by archaea and methane consumed by methane oxidizing microorganisms in the aerobic peat layers.

Fens are estimated to make up nearly half of the total global peatland area (Aselmann & Crutzen, 1989; Lamers et al., 2015) and their contribution to methane emission from peatlands to be over 80% (Aselmann & Crutzen, 1989). Especially in the northern peatlands, higher methane emissions have been measured from fens than from ombrotrophic bogs (Turetsky et al., 2014). Hence, understanding methane emission dynamics from fen ecosystems is crucial for understanding the methane emission from northern peatlands. Furthermore, as current bogs have transitioned from fens to bogs at some point of their history, understanding the Holocene greenhouse gas balance and climatic effect of peatland requires understanding of the fen emission dynamics (Mathijssen et al., 2016).

The methane emissions from wetlands have been intensively studied by chamber techniques (e.g., Bubier et al., 2005; Riutta et al., 2007; Ström et al., 2015; Whiting et al., 1991; Whiting & Chanton, 1992), and more recently also by eddy covariance method, measuring the ecosystem scale gas exchange (e.g., Brown et al., 2014; Fortuniak et al., 2017; Hargreaves et al., 2001; Hommeltenberg et al., 2014; Jackowicz-Korczyński et al., 2010; Kim, Verma, & Billesbach, 1998; Kim, Verma, Billesbach, & Clement, 1998; Kowalska et al., 2013; Mikhaylov et al., 2015; Nadeau et al., 2013; Rinne et al., 2007). While chamber measurements provide insight to many processes and to microtopography-scale spatial variability, they usually lack the temporal resolution of eddy covariance data. Also, the deployment of chamber systems to obtain long-term measurements without disturbance to studied ecosystem, such as changes in snow accumulation inside collar, warming effect of many automated chamber systems, is challenging. The eddy covariance method (e.g., Aubinet et al., 2012), which has gained popularity in recent years for measurement of methane emission from wetlands, has typically high temporal resolution due to its continuous operation and minimal disturbance to the ecosystem measured. This has led to increasing amount of continuous long-term methane flux measurements from wetlands and other ecosystems.

The methane flux measurements with higher temporal resolution have revealed partly contrasting results on the environmental controls of methane emission from different study sites. However, the exponential dependence of methane emission on peat temperature has been well documented (Jackowicz-Korczyński et al., 2010; Kim, Verma, & Billesbach, 1998; Marushchak et al., 2016; Mikhaylov et al., 2015; Rinne et al., 2007).

In part of the measurements, no simple dependence of methane flux on water table has been observed (Brown et al., 2014; Jackowicz-Korczyński et al., 2010; Rinne et al., 2007), while in others the higher methane emissions are observed during higher water tables (Mikhaylov et al., 2015). The contrasting results may be due to differences in the site characteristics and counteracting processes. As a large part of the methane emission in sedge dominated wetlands is transported via diffusion in the aerenchyma, it bypasses the potential oxidation in the aerobic acrotelm. This would lead to relative insensitivity of methane emission to water table position (WT). However, at very low WTs the roots of aerenchymatous plants do not reach the anaerobic layers inhibiting the plant mediated transport. Conversely, very high water table can submerge the above-ground parts of aerenchymatous plants, leading also to lower methane emission.

At some of the measurement sites the observed methane emission has a clear diel cycle, with higher diurnal emission (Kim, Verma, Billesbach, & Clement, 1998; Kowalska et al., 2013), while at other sites no such cycle is observed (Jackowicz-Korczyński et al., 2010; Rinne et al., 2007). The vegetation at sites with strong diel cycle of methane emission is commonly dominated by species with convective throughflow via root system, such as *Phragmites australis* (Brix et al., 1992).

While methane flux measurements with eddy covariance are now accumulating, very few published time series of methane fluxes measured by eddy covariance technique spanning over 5 years exist. Knox et al. (2016) have presented a 6.5-year time series measured at a Californian rice paddy, and Li et al. (2016) used 5 years of data from Lompolojänkkä, Finland, and 6 years from Siikaneva, Finland, to evaluate methane model performance. Also, many ecosystem scale studies on methane emission have not combined carbon dioxide fluxes in the analysis. Therefore, our knowledge on interannual variations in ecosystem scale methane emissions is limited and the relations with environmental factors have been derived from seasonal scale measurements. This might partly explain the contrasting results on environmental controls because in seasonal time scales abiotic and biotic factors that regulate methane emissions, such as temperature, water level, leaf area, and substrate availability via plant production or net ecosystem exchange (NEE), are strongly intercorrelated.

To reveal the dependencies, a longer period of measurements with a large combination of factors is needed. Recently, homogeneity of slope approach (HOS) has been used to estimate how much of the interannual variability of carbon dioxide fluxes can be explained by interannual variability of environmental variables (Hui et al., 2003; McVeigh et al., 2014; Teklemariam et al., 2010). This approach has not thus far been used for methane fluxes.

As the greenhouse gas balances, including methane emission, of northern peatlands can change either naturally (Mathijssen et al., 2016, 2017) or due to human intervention (Mathijssen et al., 2017; Petrescu et al., 2015), it is crucial to understand the dynamic responses of methane emission to abiotic and biotic drivers. Also, northern latitudes are expected to experience faster than average climate warming (IPCC, 2013), which makes this understanding even more important.

Much of previous work on the relations of methane emission and various abiotic and biotic drivers have been based on spatial variation (Bubier et al., 2005; Riutta et al., 2007; Turetsky et al., 2014; Whiting & Chanton, 1993). Consequently, relations between methane emission, GPP, and WT may be due to the different plant communities and associated microbial communities at different microtopographic features, rather than direct water table effect. Thus, the eddy covariance measurements with high temporal resolution and several years of coverage can be used to assess the validity of temporal relationships drawn from spatial variation, that is, space-for-time analogy.

We have conducted eddy covariance flux measurements of methane at a boreal wetland ecosystem since 2005, which to our knowledge constitutes at present the longest methane flux time series by eddy covariance. Our aim in this paper is to quantify the annual balances, seasonal cycles, and interannual variability of methane fluxes from this ecosystem. Furthermore, the aim is to analyze the relationships of the measured methane fluxes to the abiotic environmental conditions, as well as biotic substrate control measured as carbon dioxide fluxes, at different temporal scales. We will also use the HOS approach to estimate how much of the interannual variation can be explained by interannual variation of environmental variables.

2. Materials and Methods

2.1. Measurement Site

The data analyzed in this study were measured at a fen site at Siikaneva wetland complex in Southern Finland during years 2005–2015. Siikaneva wetland complex comprises 12 km^2 of boreal wetland, including minerotrophic and ombrotrophic areas. The oldest basal dates of the wetland complex are over 10,000 years, and the wetland has undergone considerable lateral expansion even within the last 5,000 years. Deepest peat layers of the wetland complex are over 6 m (Mathijssen et al., 2016). The climate is boreal with no permafrost, with annual average temperature of 3.3°C and annual rainfall of 710 mm during the period 1971–2000 (Drebs et al., 2002). The spring thaw typically occurs at the fen in April–May. The fen gets snow cover in November–December and freezes by the end on December. Thus, the snow and ice clad period is January–March and snow-free period June–October.

The flux measurements analyzed in this study were conducted in the minerotrophic fen part of the wetland (61°50′N, 24°12′E, 162 m above sea level). The vegetation at the site is dominated by peat mosses (*Sphagnum balticum* [Russow] Russowex C.E.O. Jensen, *Sphagnum majus* [Russow] C.E.O. Jensen, and *Sphagnum papillosum* Lindb.), Sedges (*Carex rostrata* Stokes, *Carex limosa* L., and *Eriophorum vaginatum* L.), and Rannoch rush (*Scheuchzeria palustris* L.). The measurements in this site began in 2005. The first results of eddy covariance flux measurements of carbon dioxide and methane have been published by Aurela et al. (2007) and Rinne et al. (2007), respectively. In addition, manual chamber flux measurements of carbon dioxide and methane, conducted in 2004 and 2005, as well as vegetation characteristic are described by Riutta et al. (2007). Standing plant biomass of the site is presented by Laine et al. (2012). The measurement site is a class 2 ecosystem site in the ICOS research infrastructure (https://www.icos-ri.eu/) since November 2017.

2.2. Flux Measurements

The measurements of carbon dioxide and methane exchange have been conducted nearly continuously since 2005 using the eddy covariance technique (e.g., Aubinet et al., 2012). Over the 11-year measurement period, there have been some longer data gaps and changes in the measurement setup, due to development of technology, breakage of instruments, and logistical demands. The instruments used for eddy covariance

Table 1
Instruments Used in the Flux Measurement System

Period	Sonic	CH_4 analyzer	CO_2 and H_2O anal.
2005–2007	**Metek USA-1 (a)**	**Campbell TGA-100**	**Li-Cor 7000**
2008–2009	**Metek USA-1 (a)**	**Los Gatos RMT-200**	**Li-Cor 7000**
2010	**Metek USA-1 (a)**	**Los Gatos RMT-200** Picarro G1301-f	**Li-Cor 7000**
2011	**Metek USA-1 (a)**	**Picarro G1301-f**	**Li-Cor 7000**
2012 to January 2014	**Metek USA-1 (b)**	**Los Gatos RMT-200**	**Li-Cor 7000**
2014/2 to November 2014	**Metek USA-1 (b)**	**Los Gatos GGA-24EP**	**Li-Cor 7000** Los Gatos GGA-24EP
December 2014 to April 2015	**Metek USA-1 (b)**	**Los Gatos RMT-200**	**Li-Cor 7000** Los Gatos GGA-24EP
April 2015 to September 2015	**Metek USA-1 (b)**	**Los Gatos GGA-24EP**	**Li-Cor 7000** Los Gatos GGA-24EP

Note. Instruments used in this study are indicated in bold.

measurements are listed in Table 1. There have been several changes of methane analyzer and a small change (7 m) in the location of the measurement tower in February 2010.

The different methane analyzers used at the site have been previously compared by Peltola et al. (2013, 2014). According to their results there are practically no systematic differences between the analyzers used in this study, the differences being about 4% for the seasonal methane emission. Also, the two individual sonic anemometers used were compared to each other at the site, and they are unlikely to cause a major (>10%) systematic difference in gas fluxes.

The postprocessing of the eddy covariance flux data has been done with EddyUH postprocessing software (Mammarella et al., 2016). The fluxes were calculated as half-hourly averages using block averaging, sector-wise planar fitting, and empirical high-frequency correction according to Mammarella et al. (2009).

2.3. Ancillary Measurements

The ancillary measurements conducted continuously at Siikaneva include air temperature (T_{air}) and relative humidity (Rh), surface moss temperature (T_m), peat temperatures at several depths between 5 and 50 cm in the peat profile (T_5, T_{20} T_{35}, T_{50}), photosynthetic photon flux density (PPFD), net radiation, precipitation, and WT. The zero level of the WT must be taken as indicative only, as we do not have detailed description of the microtopography of the fen surface, needed to tie the water table measurement to surface statistics. We also used temperature and precipitation data from nearest weather station (Juupajoki Hyytiälä) of Finnish Meteorological Institute, located 5 km east from the Siikaneva measurement site. Also, global radiation data from Hyytiälä were used to fill some gaps in radiation data.

2.4. Gapfilling of Carbon Dioxide Fluxes

To obtain daily, monthly, and annual values of NEE of carbon dioxide, and its subcomponents gross primary production (GPP) and ecosystem respiration (R_{eco}), previously developed and tested gap-filling methods for wetland fluxes (Aurela et al., 2001, 2007) have been applied. Prior to gapfilling, the data were filtered to remove data with stationarity test value over 1 (Foken & Wichura, 1996). Friction velocity threshold was determined based on change-point detection, similarly as in Barr et al. (2013). This analysis gave values between 0.15 and 0.17 m s^{-1} depending on which periods were used in the analysis. In general, we used 0.17 m s^{-1} as the threshold. Also, data with wind direction from pump house and instrument shelter (330°–30°) and periods when the instrumentation was malfunctioning were removed prior to analysis.

In general, the gap-filling algorithm depends on PPFD, air temperature, and WT. These parameters were measured on site. In the case of shorter data gaps in PPFD, temperature or WT missing values were gapfilled with linear interpolation. In the case of gaps longer than a couple of hours, data from Hyytiälä station (Hari & Kulmala, 2005), located 5 km to the east, were used for PPFD and temperature, whereas data from a water table measurement at the same peatland complex, about 1 km northwest (for location, see Mathijssen et al., 2016),

were used for water table data. During years 2010 and 2012 PPFD data were missing, and data from Hyytiälä station were used.

The equation used to gapfill the carbon dioxide flux time series can be written as

$$\mathrm{NEE} = \frac{\mathrm{PI} \times \alpha \times \mathrm{PPFD} \times \mathrm{GP_{max}}}{\alpha \times \mathrm{PPFD} + \mathrm{GP_{max}}} + R_0 \left[1 + \frac{b_1}{1 + \exp[(\mathrm{WT} + b_2)/b_3]}\right] \times \exp\left[E\left(\frac{1}{T_0} - \frac{1}{T_{\mathrm{air}} + T_1}\right)\right], \quad (1)$$

where NEE is the net ecosystem CO_2 exchange, GP_{max} is the gross photosynthesis rate in optimal light conditions (mg m^{-2} s^{-1}), PI is an empirically determined effective phytomass index (Aurela et al., 2001), PPFD is the photosynthetic photon flux density (μmol m^{-2} s^{-1}), α is the initial slope of GPP versus PPFD (mg μmol^{-1}), R_0 is the rate of R_{eco} at 10°C (mg m^{-2} s^{-1}), WT is water table position (cm), E is a physiological parameter (in degree Kelvin), T_{air} is the air temperature, T_0 = 56.02 K, and T_1 = 227.13 K (Lloyd & Taylor, 1994). The daily PI value was calculated by subtracting the nocturnal (PPFD $<$ 20 μmol m^{-2} s^{-1}) respiration flux from the diurnal (PPFD $>$500 μmol m^{-2} s^{-1}) flux as a 7-day running mean. During summertime (approximately from April till mid-October), E was determined by fitting the temperature to the nocturnal flux data through the year. The other model parameters b_1, b_2, and b_3 are fitted only once, while α, GP_{max}, and R_0 are fitted in biweekly periods: An R_0 value was first determined by fitting the respiration (second term in the right-hand side of equation (1)) to the nocturnal NEE for each of these periods, then the values of α and GP_{max} were obtained by fitting the NEE equations to the diurnal and nocturnal NEE. During winter when no uptake of CO_2 was observed, the gaps were filled by a running mean of 2 days. The partitioning of NEE to GPP and R_{eco} was conducted also with equation (1).

2.5. Methane Flux Analysis

The aim of our analysis was to reveal the dependencies of methane fluxes on possible driving variables at different temporal scales. These include air and peat temperature, humidity, solar radiation, WT, and GPP.

Methane fluxes at the site have earlier been shown to have no systematic diel cycle (Rinne et al., 2007). We tested this with this much larger data set. First, we calculated the mean and median diel cycles for each month using the whole data set. Second, we analyzed the environmental controls of hourly variability of the methane fluxes using generalized linear models (GLMs) by stepwise regression. To analyze the variation in time scales shorter than a day, we removed the longer-term variation by subtracting corresponding 24-hr window running-mean-average from each flux value, prior to this statistical analysis.

For analysis of seasonal and interannual variations of methane flux, we averaged the half-hourly values to daily means. Monthly mean methane fluxes were calculated using daily averages. Before averaging, the data were filtered by the above-mentioned criteria. All the daily mean methane fluxes comprising of less than 16 half-hourly values were rejected from further analysis. Similarly, the monthly mean value was rejected if it was composed of less than 10 daily values. After these criteria 53,381 half-hourly (55%), 1,572 daily (39%), and 67 monthly (51%) methane flux values remained for the analysis.

The relations of daily mean methane fluxes to various environmental parameters were first investigated by linear correlations between methane flux and these parameters. As peat temperature has been shown to exert exponential behavior to methane fluxes (e.g., Jackowicz-Korczyński et al., 2010; Kim, Verma, & Billesbach, 1998; Mikhaylov et al., 2015; Marushchak et al., 2016; Rinne et al., 2007), logarithm of methane emission was also included as a variable in correlation matrix.

In the analysis of the connection between GPP and methane emission, we evaluated the correlations at daily and monthly time scales. For the analysis of time lag between methane emission and GPP we calculated cross correlations between daily averages of fluxes with different time lags between 0 and 90 days. This analysis proceeded as follows: (1) We calculated correlation coefficient between time series by aligning the two data columns, nongapfilled daily average methane emission, and GPP, with no time lag applied. Before calculating the time lag, we removed rows in which either of the data was missing. (2) We took the original data columns, applied 1-day lag, that is, moved one column one step relative to the other. Again, before calculating the time lag, we removed rows in which either of the data was missing. (3) We repeated step 2, with applying 2-day lag. This procedure was repeated over a 90-day period, yielding a correlation coefficient for each time lag. We also performed the same analysis for temperature-normalized methane emission and GPP. For this, we

normalized the daily average methane emissions as described in section 2.5.1. Only summertime data (June–September) were used for the analysis of normalized methane emission due to high variability of normalized emission in wintertime.

We analyzed the interannual variability of methane flux and its relation to environmental parameters by two approaches. First, we correlated summer season averages from June to September of different years. In the analysis of June–September averages, only those years with monthly averages available for each of these 4 months were used (N = 5–6). We did not use any gapfilling of methane fluxes in these analyses to avoid possible self-correlations. This could occur if interannual variation of methane fluxes, gapfilled, for example, using temperature, was related to interannual variation of temperature. Second, we used HOS approach (Hui et al., 2003; see section 2.5.2). The HOS approach has previously been used to study the interannual variability of carbon dioxide fluxes at peatlands (McVeigh et al., 2014; Teklemariam et al., 2010) but not for methane. For HOS approach we used nongapfilled daily average methane fluxes.

The annual methane budgets were calculated by gapfilling the methane flux data on daily basis using the model with best correspondence with the measured data, as quantified by coefficient of determination (r^2).

In the following two paragraphs, we describe two approaches for estimating the relations of the measured daily methane fluxes to environmental parameters. First, we use heuristic approach, based on our prior knowledge on methane emissions from boreal peatlands. Second, we use a statistical approach, using GLMs created by stepwise regression.

2.5.1. Heuristic Model

In principle, an algorithm describing the dependence of methane emission on multiple environmental parameters can be written as

$$F = \prod_i f_i(x_i), \tag{2}$$

in which the flux, F, is a product of independent algorithms, f_i, for each environmental parameter, x_i. This approach is similar to the one used in emission models for nonmethane hydrocarbons from vegetation (e.g., Guenther et al., 2012). As methane emission correlated best with peat temperature at 35 cm depth, and as it has previously been shown to have an exponential relation with temperature, we fitted first an exponential function,

$$f_1(T) = a_1 e^{a_2 T}, \tag{3}$$

to the observed daily average fluxes. Here T is the peat temperature at chosen depth and a_1 and a_2 are empirical coefficients. The depth off the temperature measurement was chosen based on best correlation between temperature and methane flux. The fitting was done using nlinfit function of Matlab (R2015b).

Gross primary production can drive methane production via root exudates. Thus, we can use this as second parameter in our heuristic model. In order to remove the dominant effect of temperature on emission, we first normalized the daily average methane emission by dividing it with the temperature dependence function (equation (3)),

$$F_n = \frac{F}{f_1(T)}. \tag{4}$$

The intersite comparison by Whiting and Chanton (1992) showed linear relation between methane emission and NEP. Hence, we analyzed the relation between methane emission normalized by temperature (equation (4)) and GPP using a linear relation, in the form of

$$f_2(\mathrm{GPP}) = c_1 + c_2 \mathrm{GPP}, \tag{5}$$

where c_1 and c_2 are empirical coefficients.

As the WT is often referred to be of major importance to methane emission, we also investigated the relation of methane emission and WT. We investigated this relation both by normalizing the daily average methane emission first by temperature dependence (equation (4)) and second by normalizing with both temperature and GPP dependence.

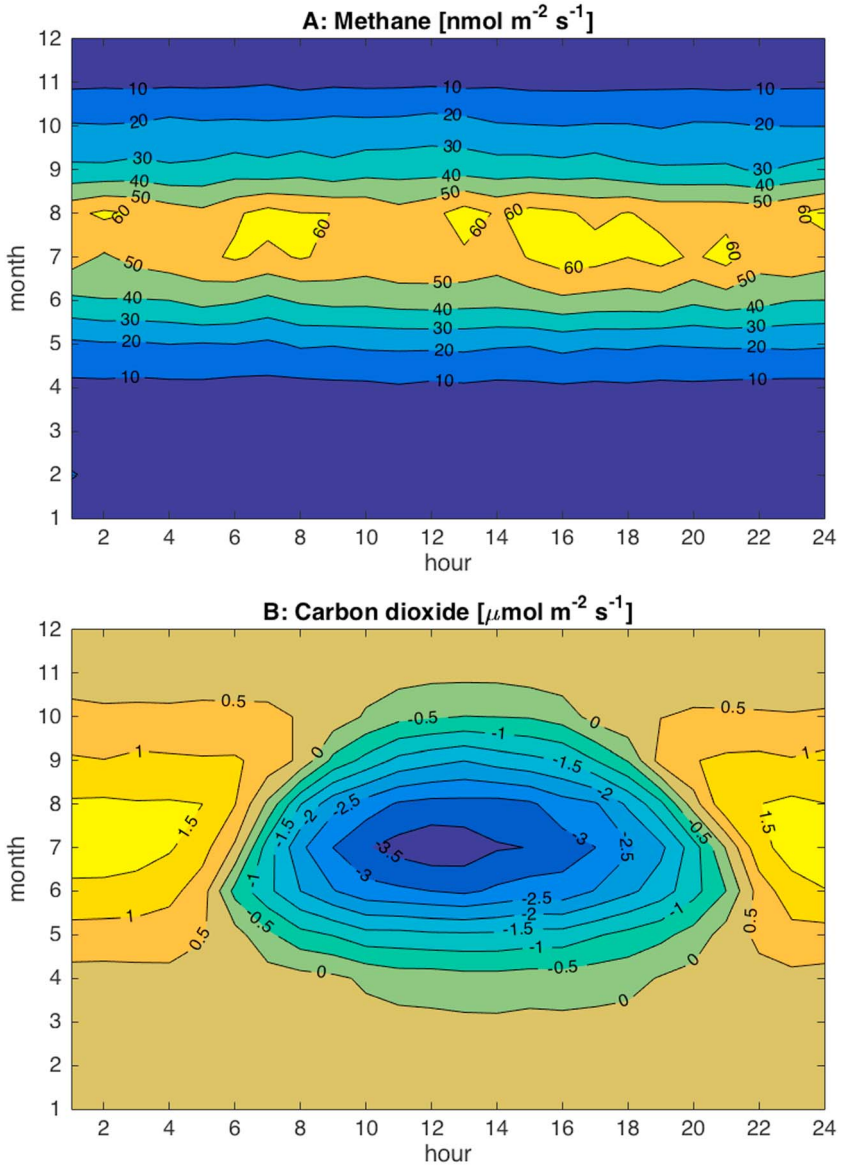

Figure 1. Seasonal and diel cycles of median (a) methane and (b) carbon dioxide fluxes, based on nongapfilled data.

Previous studies have reported, for example, methane fluxes decreasing exponentially with descending WT (Bubier et al., 2005) and unimodal relations (Turetsky et al., 2014). To better visualize the shape of the water table relation we bin-averaged the normalized daily average methane flux data according to WT to 5-cm bins. In order to avoid the effects of ice and snow cover, we used only data from June to September to derive these relations. These months have highest vascular LAI (Riutta et al., 2007) and also the highest methane fluxes.

There are likely to be various processes leading to both decrease and increase in the methane emission from fens with low WT (Raivonen et al., 2017). Review by Turetsky et al. (2014) also shows evidence on unimodal water table dependence, at least from certain types of wetlands. To mathematically describe the effects of the counteracting processes on methane fluxes, we can use two sigmoid curves, representing increase and decrease of methane emission with water table. Combining two sigmoid curves with opposite tendencies leads to an equation with expected behavior,

$$f_3(\mathrm{WT}) = \frac{b_1}{(1 + e^{b_2(\mathrm{WT}+b_3)})(1 + e^{-b_4(\mathrm{WT}+b_5)})}, \tag{6}$$

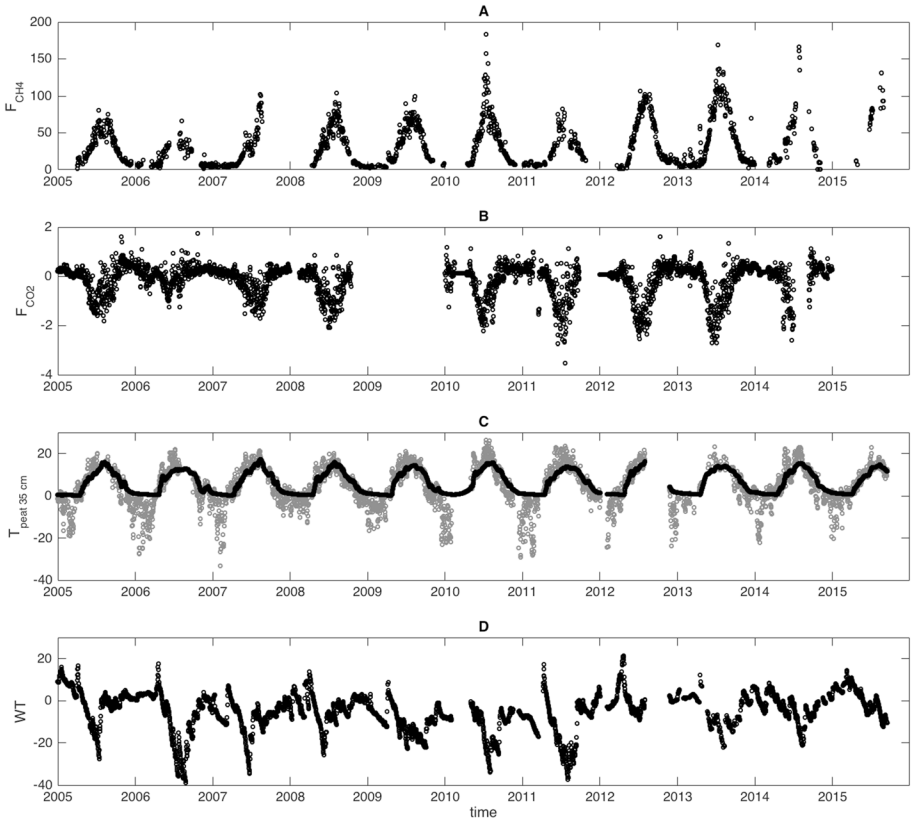

Figure 2. Time series of (a) daily averages of methane flux (nmol m^{-2} s^{-1}), (b) gapfilled daily net ecosystem exchange (μmol m^{-2} s^{-1}), (c) daily average air temperature (gray) and peat temperature at depth of 35 cm (black; °C), and (d) daily average water table position (cm).

where WT is the water table position and b_1–b_5 are empirical coefficients. In this formulation, the coefficient b_1 defines the level the sigmoid curve reaches, coefficients b_2 and b_4 defines the slope of the rising or descending part of the curve, and coefficients b_3 and b_5 the location of the rising and descending parts along WT axis. The formulation approaches zero for high and low water tables and can have asymmetric slopes across maximum of the curve, depending on coefficients b_2 and b_4. We fitted equation (6) to bin-averaged normalized methane fluxes using nlinfit function of Matlab (R2015b).

Finally, daily methane fluxes were calculated using a model comprising either one, two, or three parameters. For example, the equation comprising all three parameters is written as

$$F = f_1(T_{35})f_2(\mathrm{GPP})f_3(\mathrm{WT}), \tag{7}$$

where f_1 is equation (3), f_2 is equation (5), and f_3 is equation (6). The calculated emissions were compared to observations by goodness of fit.

2.5.2. Stepwise Regression and Generalized Linear Models

Generalized linear models describe response variable with a linear combination of functions depending on input parameters. In the case of simple model with linear responses and no interactions between variables, this can be written as

$$Y = \beta_0 + \sum\nolimits_i \beta_i X_i, \tag{8}$$

where Y is the response vector, in the case of this analysis methane flux, and X_i a column of input matrix, that is, environmental parameter. In more general case we can have interactions between

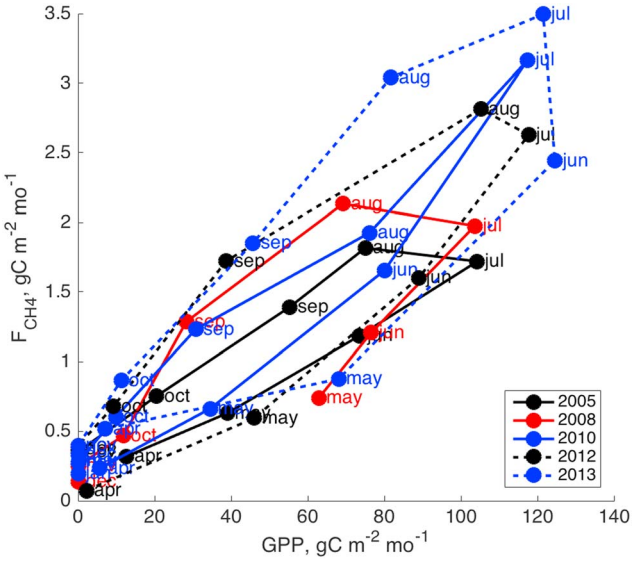

Figure 3. Monthly average nongapfilled methane emission against monthly average gross primary production.

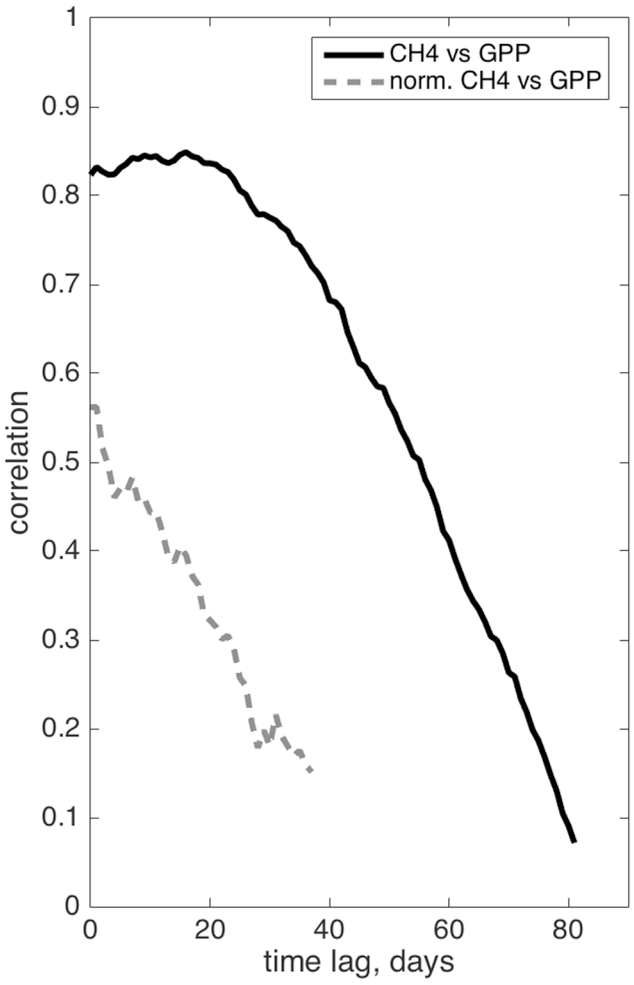

Figure 4. Correlation (r) as a function of time lag applied between time series. Only correlations with $p < 0.01$ are shown.

parameters (mathematically their products) and even interaction with categorical parameters (i.e., different slopes for observations with different categorical parameter).

We created the model using first stepwise regression (Matlab stepwiseglm) using daily average data for most parameters and daily gapfilled sums for carbon dioxide fluxes. We selected the variables to include in the stepwise regression by examining the correlation diagram. Based on correlation coefficients we first selected the parameter with highest correlation. We then excluded those that are highly correlated with the parameter selected first. After final selection of the model parameters by stepwise regression, we refitted the model using linear regression (Matlab fitglm). In order to examine seasonal differences in drivers of methane emission, we conducted the analysis also separately for snow-free season (June–October) and snow period (January–March).

2.5.3. Homogeneity of Slope Approach

We also use the GLM as a tool to investigate the interannual variability, following the approach of HOS model (Hui et al., 2003). In this approach, we used stepwise regression to create a model without year as category variable, that is, fixed slope model (section 2.5.2). As second step, we create a model using the explanatory variables of the fixed slope model but including year as categorical variable with linear regression (matlab fitglm), leading to variable slopes model. As in 2.5.2, we include interactions between parameters and allow quadratic relations. If the variable slope model is significantly better than the fixed slope model, according to F test, we interpret this difference as indicating unresolved interannual variability or "functional change" (Hui et al., 2003).

After creating and testing the models, we calculated the components of sum of squares of total deviation to quantify the sources of variation in methane fluxes. The total sum of squares difference (SS_{tot}) between the variable slope GLM and observations can be divided into its components as

$$SS_{tot} = SS_{sc} + SS_{ic} + SS_f + SS_e, \quad (9)$$

where SS_{sc} is due to seasonal variation of drivers, SS_{ic} is due to interannual variation of drivers, SS_f is unresolved interannual variation (functional change), and SS_e residual error. The formulations of these components follow those by Hui et al. (2003).

2.5.4. Gapfilling the Methane Flux Data

The gapfilling method was selected by the performance of heuristic models and GLMs. As carbon dioxide fluxes are likely to suffer partly from similar data gaps as methane fluxes, we used a hierarchy of gapfilling procedures. Accordingly, the first step of gapfilling was conducted using the model that performed best against the data. The gaps remaining after this step were filled with model that did not use, for example, carbon fluxes as input. Finally, the remaining gaps were filled with interpolation.

3. Results

3.1. Hourly Variation

The half hourly methane fluxes varied from 4.0 to 94 nmol m^{-2} s^{-1} (5% and 95% percentiles). The contour plots of carbon dioxide and methane fluxes on month-hour plane (Figure 1) show strong seasonal variation for both carbon dioxide exchange and methane emission, but no diel

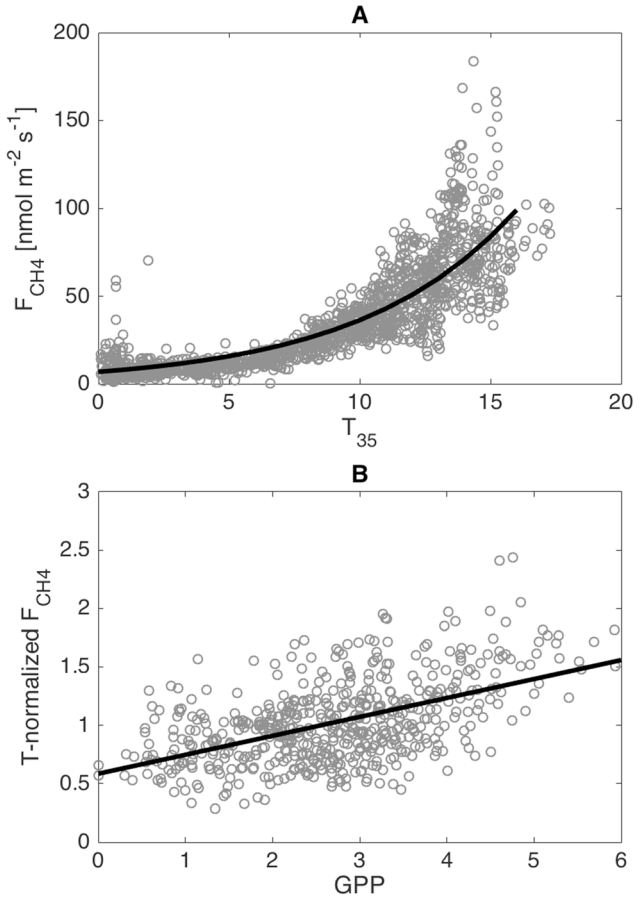

Figure 5. (a) Daily average methane fluxes against daily average peat temperature at the depth of 35 cm. The black line indicates the equation (3) fitted to the data (a_1 = 0.00682 μmol m^{-2} s^{-1}, a_2 = 0.167°C^{-1}, r^2 = 0.74). (b) Daily average temperature-normalized methane flux against gross primary production. The black line indicates linear fit to data (equation (6), c_1 = 0.585, c_2 = 0.162 [μmol^{-1} m^2 s], r^2 = 0.28).

cycle for methane flux. The GLMs created by stepwise regression for deviation of flux from its daily running mean had low explanatory power, with $r^2 < 0.1$. The full methane flux data set showed a minor diel cycle (Figure S1 in the supporting information), but removing the data obtained by Los Gatos RMT200 methane analyzer mostly removed the diel cycle (Figure 1).

3.2. Seasonal Variation

The daily averaged methane fluxes and daily average gapfilled NEE showed pronounced seasonal cycles (Figure 2), which led to significant correlations between fluxes and practically all environmental parameters (Figures 2 and S2). Methane flux correlated best with peat temperature at 35 cm depth (r = 0.82), temperature at 20 cm depth (r = 0.81), and GPP (r = 0.80). The logarithm of methane flux correlated best with temperature at 35 cm depth (r = 0.90), peat temperatures at other depths (r = 0.85–0.89), and GPP (r = 0.79). The correlation between the logarithm of methane emission and peat temperature at 35 cm depth was significantly higher than that between 5 and 50 cm (Fisher's r to z transf., $p < 0.01$) but did not differ significantly from that between 20 cm. However, for all individual years except 2011, the best correlation was found for peat temperature at 35 cm depth. The average seasonal cycle of methane emission showed maximum emissions in July and August (average 73 nmol m^{-2} s^{-1}), with small but positive fluxes also during winter (January–March average 6.7 nmol m^{-2} s^{-1}). While air temperature was typically well below zero in winter, and the surface of the peatland freezes to the depth of about 20 cm, the peat temperature at the depth of 35 cm stayed positive throughout the winter. The lowest WTs were observed in summer, but the interannual variation was large. The average water table during the measurements was −5 cm, and the average during ice- and snow-free June–September period was −13 cm, referenced to a somewhat arbitrary reference point (see section 2.3). During some years but not all, a small methane burst connected to thaw period in spring was observed (Figure S2).

Gross primary production had a high correlation with methane flux (Figure S2). By averaging the data to monthly averages, we observe a hysteresis-like behavior (Figure 3), with methane emission lagging behind GPP. The lag-time analysis (Figure 4) showed the correlation between methane emission and GPP to have a broad peak at lag times of 5–20 days. However, methane flux normalized by its temperature dependence did not show similar time lag (Figure 4).

3.3. Heuristic Model

The daily average methane emission against peat temperature at the depth of 35 cm showed exponential behavior (Figure 5a). Equation (3), fitted to the data, described the methane fluxes with r^2 = 0.73 (Figure 7a). The apparent Q_{10} obtained by fitting to the whole data set was 5.3, with annual values ranging from 3.8 to 12. The methane emission normalized by equation (4) showed positive correlation with GPP (Figure 5b; r = 0.53, $p < 0.01$). There was practically no correlation between WT and methane flux. However, bin-averaged data suggest a nonmonotonous relation to WT (Figure 6a). Especially, after normalizing the methane emission with temperature (equation (3)) and GPP (equation (5)), we observe mostly no dependence on water table, except for the very lowest and highest WTs (Figures 6b and 7).

The inclusion of GPP by linear equation (equation (5)) improved the correspondence of model to data (r^2 = 0.80), but inclusion of WT (equation (6)) did not improve the correspondence, with r^2 = 0.74 for T-WT algorithm and r^2 = 0.80 for T-GPP-WT algorithm.

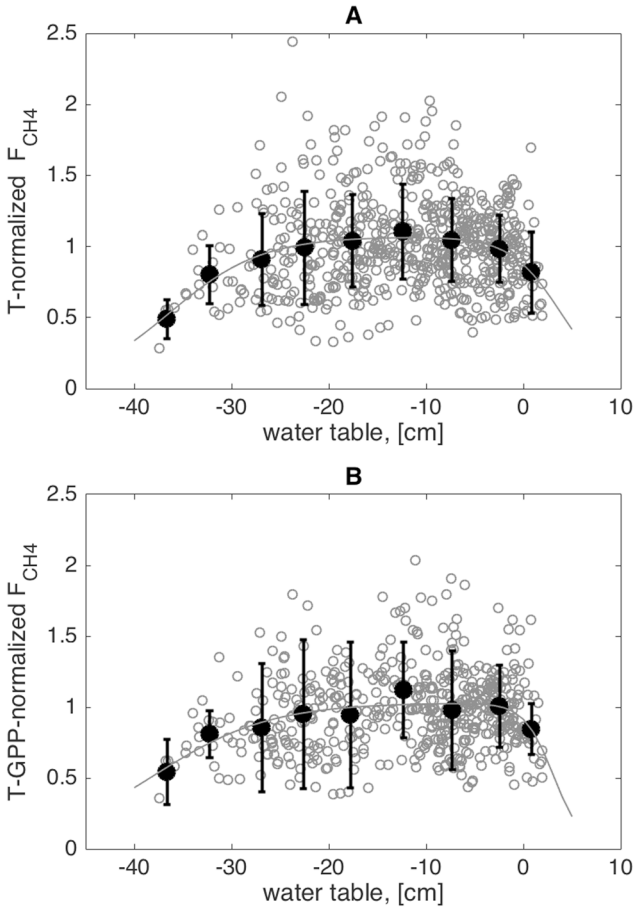

Figure 6. (a) Daily average temperature-normalized methane flux normalized, together with bin-averages, against water table position. The black line indicates equation (5) fitted to bin-averages (b_1 = 1.07; b_2 = 0.388 cm^{-1}; b_3 = −3.83 cm; b_4 = 0.213 cm^{-1}; b_5 = 36.3 cm, r^2 = 0.06). (b) Daily average temperature-gross primary production-normalized methane flux normalized, together with bin-averages, against water table position. The black line indicates equation (5) fitted to bin-averages (b_1 = 1.03; b_2 = 0.666 cm^{-1}; b_3 = −3.10 cm; b_4 = 0.168 cm^{-1}; b_5 = 38.0 cm, r^2 = 0.06).

3.4. Generalized Linear Models

The GLMs in annual basis were created by stepwise regression using the parameters shown in the Table 2. The first parameter that was selected by the stepwise regression algorithm was peat temperature, and the second one was GPP. The final fixed slopes model covering full annual cycles can be written as

$$\ln F = \beta_0 + \beta_1 T + \beta_2 \mathrm{GPP} + \beta_3 T\ \mathrm{GPP} + \beta_4 T^2 + \beta_5 \mathrm{GPP}^2, \quad (10)$$

with coefficients in Table 3.

The variable slope model for full annual cycles, created using the same explanatory parameters as the fixed slopes model but with year added as categorical variable, can be written as

$$\ln F = \beta_0 + \beta_1 T + \beta_2 \mathrm{GPP} + \beta_3 T\ \mathrm{GPP} + \beta_4 T^2 + \beta_5 \mathrm{GPP}^2 + \sum\nolimits_{\mathrm{yr}} \left(\beta_{6,\mathrm{yr}} + \beta_{7,\mathrm{yr}} T_{\mathrm{yr}} + \beta_{8,\mathrm{yr}} \mathrm{GPP}_{\mathrm{yr}}\right). \quad (11)$$

Thus, both models include peat temperature (35 cm) and GPP as drivers. These models correspond to the observed fluxes well, with r^2 = 0.84 for fixed slope model and r^2 = 0.89 for variable slope model (Figure 8). The variable slope model was significantly better according to F test ($p < 0.01$).

As the snow-free period (June–October) methane fluxes correlated best with the temperature at 20 cm, we used this for GLM for summer. For the snow-free period the stepwise regression selected peat temperature as the first explanatory variable and GPP the second. As for the whole year, the inclusion of year as category variable leads to variable slope model that was significantly better than the fixed slope model. Although the parameters in both models were the same for the summer time and whole year, the formulations were slightly different.

Wintertime (January–March) methane emissions were very small. Fixed slope GLM created with stepwise regression included peat temperature as parameter, but the explanatory power of the model was very low (r^2 = 0.16). The variable slope GLM had only year as parameter and was significantly better with r^2 = 0.42.

3.5. Gapfilling and Annual Fluxes

Based on the performance of the heuristic model and GLM, we chose to gapfill the methane fluxes using mainly GLMs. As the best performing model was the variable slope model with peat temperature, GPP, and year as variables, we used this as first step. As second step, we used a variable slope model that did not employ GPP but used other variables (air temperature, global radiation, and peat temperature). Third step did not use global radiation as this parameter was missing during one period. Finally, remaining gaps were filled by linear interpolation. The measured daily average data covered 48% of the period 2005–2014. First step increased data coverage to 86%, second to 90%, and third to 94%, with remaining 6% filled up with interpolation. The gapfilled methane flux time series is shown in Figure 9. The average annual methane emission with standard deviation was 9.7 ± 2.5 gC m^{-2}. 88 ± 3% of the annual emission occurred in May–November, which are mostly snow and ice free. 6 ± 2% occurred in snow and icebound January–March. The annual and monthly values are listed in Tables 4 and S3 in the supporting information. Annually, the methane emission was 2.7 ± 0.4% (mean ± standard deviation) of GPP. Over 10 years, methane emission was 18% of the NEE.

3.6. Interannual Variation

The annual cumulative methane flux varied from 6.0 to 14 gC m^{-2}, while the mean annual NEE, GPP, and R_{eco} were −54 gC m^{-2} (−96 to 27 gC m^{-2}), 390 gC m^{-2} (260–460 gC m^{-2}), and 330 gC m^{-2} (290–390 gC m^{-2}),

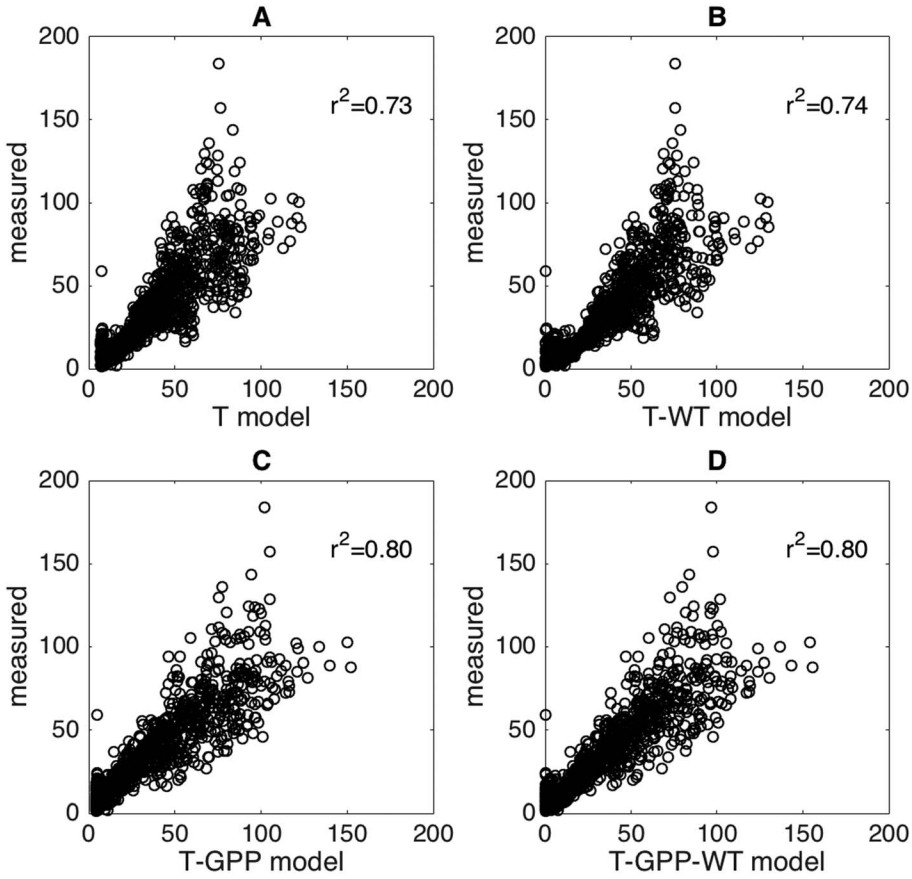

Figure 7. Performance of heuristic models against data. (a) Temperature algorithm. (b) Temperature-water table algorithm. (c) Temperature-gross primary production (GPP) algorithm. (d) Temperature-GPP-water table algorithm.

respectively. The relative variations of these fluxes, expressed as coefficient of variation (standard deviation of the annual flux, divided by the mean of annual fluxes), were 0.25, 0.73, 0.17, and 0.13 for methane emission, NEE, GPP, and R_{eco}, respectively.

Table 2
Parameters Used in Stepwise Regression to Generate the Generalized Linear Model

Model	Parameters
Whole period	Air temperature
	Vapor pressure deficit
	Global radiation
	Peat temperature at 35 cm
	Water table position
	Gross primary production (GPP)
Snow-free period	Air temperature
	Vapor pressure deficit
	Global radiation
	Peat temperature at 20 cm
	Water table position
	GPP
Winter	Air temperature
	Vapor pressure deficit
	Global radiation
	Peat temperature at 35 cm

The interannual variation of seasonal nongapfilled June–September methane emission showed significant correlation with only GPP (r^2 = 0.78, p = 0.046, Figure 10). Correlations with other parameters (peat temperature, WT, and NEE) were not significant.

The HOS analysis showed that the variable slope model performed significantly better than fixed slope model (F test, $p < 0.01$) for both the whole annual cycle and for summertime only. On the annual scale, the seasonal variation (SS_{sc}) explained 79% of the sum of squares variation, the interannual variation due to variation in explaining factors (SS_{ic}) 7.0%, interannual variation not accounted for by explaining factors (functional change, SS_f) 5.3%, and random variation (SS_e) 9.1%. Thus, 43% of the interannual variability was due to functional change.

4. Discussion

4.1. Temporal Variation of Methane Fluxes

The measured methane fluxes showed pronounced annual cycles over the measurement period, but no diel cycle. The diel cycle shown by the whole data set (Figure S1) is likely to be mostly an artifact created with imperfect

Table 3
Coefficients for Fixed Slope and Variable Slope Generalized Linear Model for the Whole Measurement Period

Fixed slope model, equation (10)			Variable slope model, equation (11)		
	Coefficient	*p*-value		Coefficient	*p*-value
β_0	−5.2286		β_0	−4.9533	
β_1	0.10721	9.3×10^{-13}	β_1	0.086069	5.3×10^{-7}
β_2	0.36583	9.5×10^{-10}	β_2	0.35254	9.8×10^{-9}
β_3	−0.032327	3.0×10^{-5}	β_3	−0.021952	0.0034
β_4	0.0044326	0.00095	β_4	0.0033769	0.016
β_5	0.036195	0.0021	β_5	0.021844	0.035
			$\beta_{6,2006}$	−0.26346	0.00062
			$\beta_{6,2007}$	−0.38856	3.0×10^{-8}
			$\beta_{6,2008}$	−0.27619	0.019
			$\beta_{6,2010}$	−0.079762	0.45
			$\beta_{6,2011}$	0.03737	0.68
			$\beta_{6,2012}$	−1.2885	6.3×10^{-38}
			$\beta_{6,2014}$	0.38364	7.6×10^{-6}
			$\beta_{7,2006}$	−0.039734	0.059
			$\beta_{7,2007}$	−0.0024854	0.88
			$\beta_{7,2008}$	0.05356	0.00026
			$\beta_{7,2010}$	0.0094902	0.57
			$\beta_{7,2011}$	−0.015824	0.27
			$\beta_{7,2012}$	0.11631	2.8×10^{-8}
			$\beta_{7,2014}$	0.0022082	0.89
			$\beta_{8,2006}$	0.27084	0.0025
			$\beta_{8,2007}$	0.059658	0.39
			$\beta_{8,2008}$	−0.15737	0.0020
			$\beta_{8,2010}$	0.018061	0.73
			$\beta_{8,2011}$	−0.018087	0.73
			$\beta_{8,2012}$	−0.04172	0.54
			$\beta_{8,2014}$	−0.12246	0.032

density correction to Los Gatos RMT200 data by WPL approach (Webb et al., 1980). As Campbell TGA-100 dried the sample airstream, and Picarro G1301-f and Los Gatos GGA-24EP measured water vapor in their optical cell, enabling point-by-point density calculation, using the data from these analyzers leads to no systematic diel cycle (Figure 1). Our analysis with stepwise regression did not show any clear relation of methane fluxes at hourly time scales and any environmental parameters. The sedge dominated fens have different emission dynamics than Phragmites dominated wetlands (Kim, Verma, Billesbach, & Clement, 1998; Kowalska et al., 2013). The apparent diel cycle of the data measured with LGR RMT200, probably due to water vapor related density and line broadening effects, is a relatively minor one. As the quality control routines employed in eddy covariance data processing are more likely to remove nocturnal measurements, the daily emission derived using simple daily averages may be an overestimate. However, calculating the monthly average emission from medians in Figure S1 using 8 afternoon hours leads to overestimations that are below 10% for all months except May, when the overestimation was 12%. Carbon dioxide fluxes observed here showed diel and annual cycles characteristic to boreal ecosystems (e.g., Aurela et al., 2007; Suni et al., 2003), with uptake during summer days and release to the atmosphere during night and winter (Figure 1b).

The spring pulse, when observed, was small in relation to the summertime fluxes, similar to the observations previously reported at the same site by Rinne et al. (2007) and at a boreal peatland in Komi Republic of Russian Federation by Mikhaylov et al. (2015). This modest magnitude contradicted with Hargreaves et al. (2001), who observed a significant fraction of annual methane emission from subarctic Kaamanen mire to be emitted during spring pulse. The importance of spring pulse may indeed be higher at more northern sites, such as Kaamanen, with deep frozen layer in winter. In south-boreal Siikaneva, with only about 20-cm frozen layer, much of the methane produced in wintertime may escape through ice and snow, as the frozen layer in peatlands is more porous than, for example, lake ice, containing in many places frozen plant parts, such as

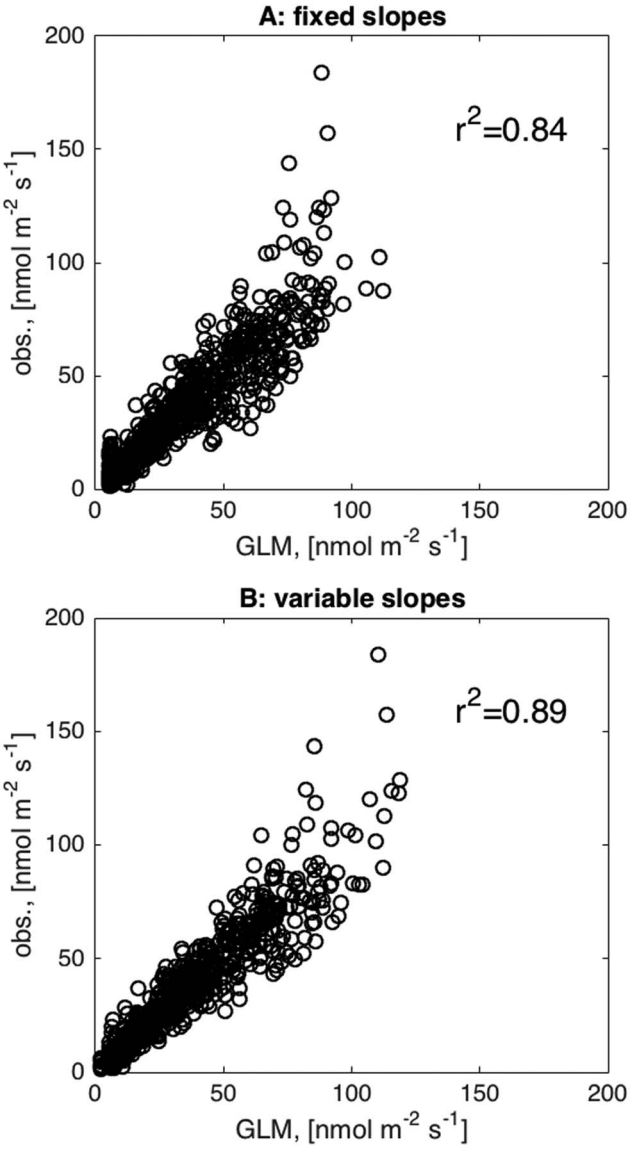

Figure 8. Performance of generalized linear models against data. (a) Fixed slope model. (b) Variable slope model.

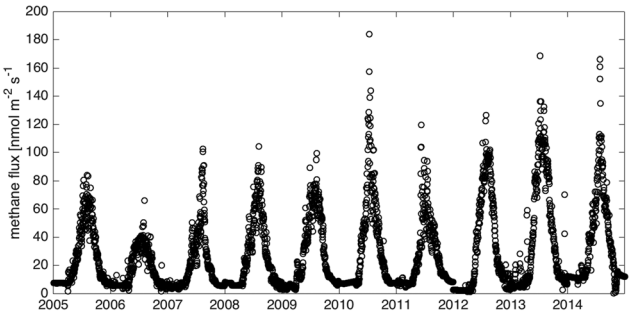

Figure 9. Time series of gapfilled daily average methane flux.

moss and sedges. Still, emission during the summertime clearly dominated the annual emission, with emission of snow and ice clad period being of minor importance.

4.2. Relation of Methane Flux to Environmental Parameters

Daily average methane fluxes correlated significantly with air temperature and peat temperature measured at different depths, as well as other abiotic parameters (Figure S2). These parameters also show highly significant correlations with each other, indicating largely coherent seasonal cycles.

The highest correlations were observed between logarithm of methane flux and peat temperatures at 20–35 cm depth, similarly to the earlier observation at the site by Rinne et al. (2007). This is in line with the common observation of relation of methane emission on temperature being exponential (e.g., Jackowicz-Korczyński et al., 2010; Kim, Verma, & Billesbach, 1998; Kim, Verma, Billesbach, & Clement, 1998; Marushchak et al., 2016; Mikhaylov et al., 2015). The temperatures at different depths of peat layer have effects on different processes leading to net methane emission. For example, temperature responses of methane production and consumption differ from each other (Dunfield et al., 1993) which can lead to confounding effects on observed temperature relations. Consequently, the statistical response of measured net methane emission to temperature does only quantify link empirically, but does not disentangle the underlying mechanisms.

In the previous study using data from 2005 at the site by Rinne et al. (2007), exponential relation between methane emission and peat temperature was observed at temperatures below 12°C, with no correlation above 12°C. By using the current 11-year data set, the exponential relation between peat temperature and methane flux was confirmed for the whole temperature range, with no upper limit (Figure 5). The reason for the lack of temperature relation above 12° in year 2005 may be related to rapid ascent of water table at the onset of peat temperatures above 12°C.

The values of Q_{10} presented in results were calculated from seasonal time series and are affected by confounding factors, such as phenology. Thus, we refer to them as apparent Q_{10}. While part of the apparent Q_{10} is likely to be due to the confounding factors, the temperature is also likely to have a direct effect on the metabolic activity of methane producing Archaea. The published apparent Q_{10} values of methane fluxes, measured by eddy covariance, range from 2.4 to 6.6 (Table 5). The apparent Q_{10} of the whole data set presented here, 5.3, is within the range of these, although the interannual variation is large. We should note that different studies have correlated the methane fluxes with temperature measured at different depths, which affects the apparent Q_{10} values. For example, with our data the apparent Q_{10} using peat temperature at 5-cm depth would have been 3.1. Thus, difference between Q_{10} obtained from different sites may reflect the differences of peat temperature measurements. However, the interannual or seasonal variations in the Q_{10} may be due to variations in other controlling factors.

Water table has been commonly indicated to be one of the major controls of methane emission (e.g., Bubier et al., 2005; Turetsky et al., 2014). However, in some studies on temporal behavior of ecosystem scale methane emission, no clear dependence of methane fluxes on WT has been observed (e.g., Jackowicz-Korczyński et al., 2010; Rinne et al., 2007).

Table 4
Annual Cumulative Values of Methane Emission (F_{CH4}), Net Ecosystem Exchange (NEE), Gross Primary Production (GPP), and Ecosystem Respiration (R_{eco})

	F_{CH4} gC m^{-2}	Q_{10}	NEE gC m^{-2}	GPP gC m^{-2}	R_{eco} gC m^{-2}	T_{ave} °C	Precip. mm
2005	9.0	3.8	−29	380	350	4.4	703
2006	6.0	4.4	27	260	290	4.6	653
2007	7.0	5.9	−48	350	290	4.5	700
2008	8.9	5.2	−78	370	300	4.9	933
2009	9.6	5.9	N.A.	N.A.	N.A.	3.8	502
2010	11	5.8	−58	350	310	2.5	657
2011	8.8	4.5	−60	450	390	4.9	745
2012	11	6.6	−96	410	300	3.2	907
2013	14	12	−85	460	370	4.9	615
2014	12	11	N.A.	N.A.	N.A.	5.1	579
2015	N.A.	6.1	N.A.	N.A.	N.A.	5.5	658

Note. Annually derived Q_{10}. Mean annual temperature (T_{ave}) and annual cumulative precipitation (Precip.) at Juupajoki Hyytiälä weather station.

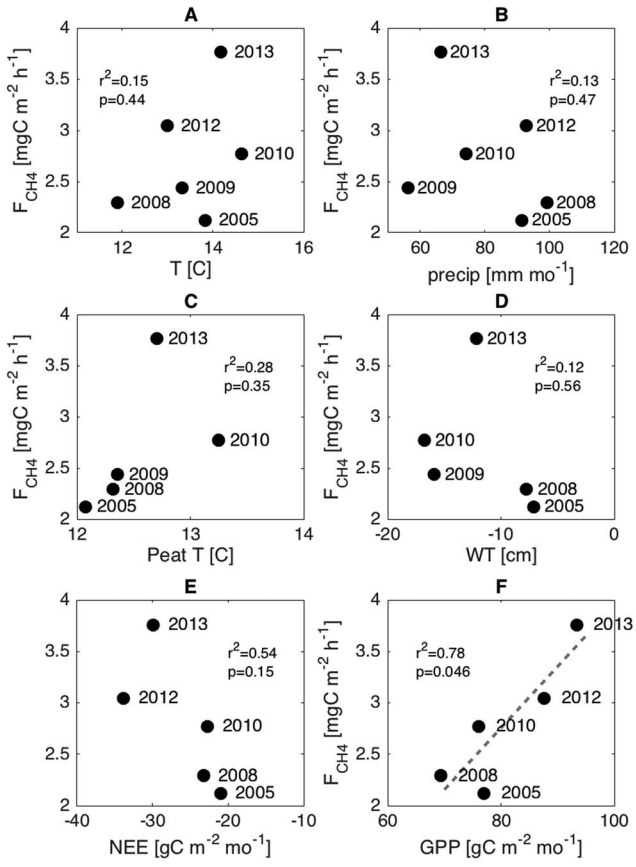

Figure 10. June–September nongapfilled average methane flux against (a) air temperature (°C) at Hyytiälä Juupajoki weather station, (b) precipitation (mm mo^{-1}) at Hyytiälä Juupajoki weather station, (c) peat temperature (°C) at 35 cm depth, (d) water table position (cm), (e) net ecosystem exchange (gC m^{-2} mo^{-1}), and (f) gross primary production (GPP; gC m^{-2} mo^{-1}). The regression line (F_{CH4} = 0.0600 × GPP − 2.0420 mgC m^{-2} h^{-1}) is included in (f), where the correlation is significant.

Our analysis also shows no clear dependence of methane emission on water table, but the bin averaged data suggest a broad maximum of methane fluxes at intermediate WTs between about −25 cm and −5 cm, with a slight decrease of emission both with low and high water tables (Figure 6). As water table was between these values for most of the snow-free period, the water table did not have a major effect on temporal variation of methane emissions. These water table limits must be taken as indicative only, as the zero level of water table is not quantitatively tied to surface microtopography statistics. Similar unimodal behavior of methane emission with water table was obtained by annual GLM without year as category parameter. The observed water table dependence is qualitatively similar to that of NEE as observed by Aurela et al. (2007).

There are likely to be various processes leading to decrease in the methane emission from fens with low WT. For example, as WT descends, a considerable part of roots of aerenchymatous plants may not reach the anaerobic water saturated peat, thus inhibiting this transport route to the atmosphere. According to Saarinen (1996) majority of roots of many vascular plants in peatlands are in quite shallow layer (0–30 cm), although part of the root system reaches much deeper. The increased oxidation in the diffusion pathway within nonsaturated peat is likely to increase this effect. Thus, if the water table were drawn much lower than observed during the 10-year period reported here, the methane emission would be inhibited more, and the peatland could even turn to a small sink of methane at extremely low WT.

On the other hand, there can be at least two mechanisms that can lead to lower methane emissions with very high water table. First, increasing water table may lead to total submersion of aerenchymatous plants at hollows and lower lawn surfaces, leading to decreasing fluxes with ascending water table. The review by Turetsky et al. (2014) point out to low emission from flooded sites. Second, if the ascend of water table is due to rain at the site, it may create a layer of water with low dissolved methane concentration on top of peat water with higher concentration. This may slow down the diffusion through peat matrix in the topmost peat layers, as the diffusion in water is slower than in air-filled pores.

The relative insensitivity of methane flux to WT within the range observed in this study may indicate a small contribution of methane oxidation as control of methane emission from sedge fens. This may be due to abundant aerenchymatous vascular plant cover at this type of peatlands, which leads to most of the methane to be emitted through the aerenchyma. Thus, the methane bypasses the aerobic peat and moss layers for the typical range of WTs.

The fundamental difference of the water table relation derived here, and those represented by, for example, Bubier et al. (2005), Riutta et al. [2007], and Turetsky et al. (2014), is that the one presented here concerns temporal variability on subannual time scale, while those mentioned above refer mostly to spatial variability. In the latter, the plant community composition, that is, abundance of aerenchymatic plants and dwarf shrubs, may play an important role in either promoting or inhibiting the methane emission (Joabsson et al., 1999; Wang et al., 2015), and thus, it is not obvious that the space-to-time analogy is applicable to seasonal time scales.

Even though the methane is strongly correlated with temperature on a seasonal time scale, their interannual variation does not show significant

Table 5
Published Apparent Q_{10} Values Based on Temporal Variability of Ecosystem Scale Emission

Reference	Ecosystem	Depth of temperature measurement	Q_{10}
This study	Boreal fen	35 cm	5.3 (3.8–12)
Kim, Verma, and Billesbach (1998)	Temperate midlatitude marsh	Average of top sediment 0–15 cm, under 0.4–0.6 m of water	4.4–6.6
Jackowicz-Korczyński et al. (2010)	Subarctic mire	3 cm	3.3–5.3
Mikhaylov et al. (2015)	Boreal peatland	15 cm	4.3
Marushchak et al. (2016)	Subarctic wet tundra	25 cm	2.4

correlation. This may be partly due to the smaller data set, 5 years, for June–August period. Furthermore, the maximum interannual variation of peat temperature at 35 cm depth was only 1.2°C.

4.3. Relation Between Methane Emission and Carbon Dioxide Fluxes

As methanogenic *Archaea* use mostly relatively fresh root exudates as substrate to methane production (Chanton et al., 1995; Couwenberg & Fritz, 2012; Ström et al., 2003; Whiting & Chanton, 1993), a link between carbon dioxide uptake and methane emission can be expected (Joabsson & Christensen, 2001). The methane fluxes indeed showed correlation with GPP, with hysteresis-like behavior (Figure 3). Following leaf area development typical to boreal peatlands (Wilson et al., 2007) and high availability of light in the early summer, GPP increases rapidly, but methane emission increases at much slower rate. In the late summer GPP decreases rapidly, but methane emission continues at a relatively high rate.

The lag times between the methane emission and GPP, as shown by the cross-correlation analysis (Figure 4), were on average 15 days with quite broad peak between about 5 and 25 days. However, temperature-normalized methane emission did not show any correlation lag. Thus, the lag between GPP and methane emission is likely to be due to lag between the environmental parameters controlling the GPP and those controlling methane emission, in the seasonal scale. GPP is controlled largely by PPFD and air or surface temperature, while methane emission by the temperature control and substrate availability of archaea metabolism. Incubation experiments show increased methane production with increasing temperature indicating temperature control (e.g., Juottonen et al., 2008). The significant correlation of temperature-normalized methane emission with GPP indicates that the fresh substrate input is an important controlling factor of methane emission. A rapid link between photosynthesis and methane emission has been shown in pulse labeling experiments, where ^{14}C label appeared onto emitted methane in less than 1 day (King et al., 2002; King & Reeburgh, 2002). The difference between these studies and the one reported here is that labeling experiments show when labeled carbon first appears into emitted methane, while our analysis shows the differences in the seasonal cycles of methane emission and GPP.

The interannual variation of methane emission was significantly correlated to that of GPP, when analyzed for the summer season (June–September). This, together with published observations on ^{14}C labeling (King et al., 2002; King & Reeburgh, 2002), indicates a causal dependence of seasonal methane emission

Table 6
Mean Annual Methane Emission (F_{CH4}), Net Ecosystem Exchange (NEE), Gross Primary Production (GPP), and Their Ratios Obtained by This Study, With Values Reported in Literature

Site	Type	Cite	F_{CH4} gC m^{-2}	NEE gC m^{-2}	GPP gC m^{-2}	R_{eco} gC m^{-2}	F_{CH4}/NEE	F_{CH4}/GPP
Siikaneva fen	Fen	This study	9.7	−54	380	330	18%	2.7%
Biebrza Valley	Disturbed fen	Fortuniak et al., 2017	18	−210	n.a.	n.a.	8.6%	n.a.
Federseemoor	Phragmites fen	van den Berg et al., 2016	23	−240	850	610	9.4%	2.7%
Forsinard	Bog	Levy & Gray, 2015	4.3	−110	575	460	3.9%	0.75%
Schechenfilz	Forested bog	Hommeltenberg et al., 2014	5.3	−62	n.a.	n.a.	8.6%	n.a.
Bog lake	Fen	Olson et al., 2013	16	−35	n.a.	n.a.	46%	n.a.
Samoylov Island	Wet polygonal tundra	Wille et al., 2008	2.4	−20	n.a.	n.a.	12%	n.a.
Mer Bleue	Bog	Roulet et al., 2007	3.7	−40	n.a.	n.a.	9.2%	n.a.

on photosynthesis as carbon input. The correlation of temperature-normalized methane flux with GPP (Figure 5) indicates also that the correlation between methane emission and GPP in the seasonal time scale is not purely a result of collinearity of GPP and peat temperature.

The ratio of methane emission to GPP was in the same range as obtained by intersite comparison by Whiting and Chanton (1993). The methane emission to GPP ratio (F_{CH4}/GPP), if shown to hold for a range of peatlands, could be a useful constrain for regional and global peatland methane emissions. Unfortunately, few sites report data to enable comparisons of methane F_{CH4}/GPP ratios in ecosystem scale (Table 6). The methane flux at Siikaneva was 18% of the NEE. This is higher than in the other sites listed in Table 6. However, these sites were mostly ombrotrophic peatlands with one disturbed fen. Thus, the difference of F_{CH4}/NEE is likely to be due to ecosystem type.

The observed links between methane emission and GPP are crucial for development of process-based methane emission models. In such models the methane production typically depends on the available carbon pool development (Li et al., 2016; Oikawa et al., 2017; Raivonen et al., 2017; Tian et al., 2010; Walter & Heimann, 2000; Wania et al., 2010; Watts et al., 2013; Zhuang et al., 2004), in line with our findings. Also, the possibility to remotely observe abiotic and biotic parameters controlling the carbon dioxide exchange of wetland ecosystems (Aurela et al., 2004; Lees et al., 2018; Rinne et al., 2009) may be linked to methane emissions from northern peatlands. However, in order to better understand the dynamic links between carbon dioxide fluxes and methane emission, measurements of seasonal development of substrate and dissolved methane pools within anoxic peat layers would be crucial.

4.4. Emission Algorithms

The two approaches we used to create emission parameterization for daily average methane fluxes, the heuristic and stepwise regression, showed similarities in the driving parameters. Both lead to algorithms in which peat temperature had a strong exponential control on calculated emission, with further control by GPP. The effect of WT, if included in a model, was very small or nonexistent.

The usefulness of the models with GPP as explanatory variable in gapfilling is somewhat limited. NEE measurements suffer from many of the same limitations as methane flux measurements, commonly reducing data coverage and requiring further use of gapfilling algorithms to obtain daily GPP values. Thus, in many cases, gapfilling with temperature and possibly water table algorithm is more feasible.

The GLMs explained the observed variation in methane emission better than heuristic model, especially when letting the slopes vary between years. The latter may be somewhat more transparent and can be modified based on knowledge from external studies.

4.5. Interannual Variation

The relative interannual variability of methane emission from the fen ecosystem was slightly higher than those of GPP and R_{eco}, but much less than that of NEE. As indicated by HOS analysis and significant correlation of June–September methane emission with GPP, a part of this interannual variability is related to interannual variability of GPP. The HOS approach indicated that more than half of the interannual variability was accounted for by the interannual variation of GLM drivers, peat temperature, and GPP.

The interpretation of the HOS result, as applied here to methane emission, is different than the analyses earlier conducted for carbon dioxide (Hui et al., 2003; McVeigh et al., 2014; Teklemariam et al., 2010). In those studies, only climate parameters were used as drivers, whereas for methane, GPP is indicated to be the second most important driver of methane emission by stepwise regressions. GPP is not a climate variable, but itself a result of ecosystem functioning. Thus, the interpretation of interannual variability of methane emission due to functional change of the ecosystem differs from that of the studies for carbon dioxide. We may interpret this as functional change in the methane production and oxidation processes.

5. Conclusions

A decade-long data set on ecosystem scale methane emission, measured by the eddy covariance technique, showed strong seasonal cycle but no systematic diel cycle. Daily average methane emission related mostly to peat temperature and GPP. Water table had no significant effect to methane fluxes for the observed WT range. This indicates that space-for-time analogy, commonly used upscale spatial chamber data

temporally, is not necessarily applicable in seasonal time scales. The variation of methane emission in time scales shorter than 1 day did not show strong relations with any environmental variables.

The observed relations suggest that methane emission is strongly regulated by temperature controlling, for example, the metabolic rates of methanogenic Archaea, and by carbon input via GPP. The observed close link between GPP and methane emission is crucial for development of process-based methane emission models. Methane oxidation does not seem to be an important control of variations in methane emission for the typical WT range, as water table did not show strong relation with methane emission.

The interannual variation of summertime methane emission correlates with that of GPP. The HOS approach showed that interannual variation of GPP, temperature, and other meteorological parameters were not able to fully explain the interannual variability of methane emission. On the annual scale, the seasonal variation (SS_{sc}) explained 79% of the sum of squares variation, the interannual variation due to variation in explaining factors (SS_{ic}) 7.0%, interannual variation not accounted for by explaining factors (functional change, SS_f) 5.3%, and random variation (SS_e) 9.1%. Thus, 43% of the interannual variability was due to functional change.

Acknowledgments
The study was supported by the National Centre of Excellence (272041), ICOS-Finland (281255), and CARB-ARC (286190). T. Vesala was supported by an Academy professor project (284701) funded by the Academy of Finland, and E.-S. Tuittila by Academy of Finland project SA287039. We thank Pauli Jokela at the Finnish Meteorological Institute for climate data from Juupajoki Hyytiälä station. We also thank the two anonymous reviewers for their thorough and constructive reviews. The data are available at AVAA data platform http://avaa.tdata.fi/web/smart/smear.

References

Aselmann, I., & Crutzen, J. P. (1989). Global distribution of natural freshwater wetlands and rice paddies, their net primary productivity, seasonality and possible methane emissions. *Journal of Atmospheric Chemistry*, *8*(4), 307–358. https://doi.org/10.1007/BF00052709

Aubinet, M., Vesala, T., & Papale, D. (Eds.) (2012). *Eddy covariance—A practical guide to measurement and data analysis*. Dordrecht: Springer. 978-94-007-2350-4

Aurela, M., Laurila, T., & Tuovinen, J.-P. (2004). The timing of snow melt controls the annual CO_2 balance in a subarctic fen. *Geophysical Research Letters*, *31*, L16119. https://doi.org/10.1029/2004GL020315

Aurela, M., Riutta, T., Laurila, T., Tuovinen, J.-P., Vesala, T., Tuittila, E.-S., et al. (2007). CO_2 balance of a sedge fen in southern Finland—The influence of a drought period. *Tellus Series B*, *59*, 826–837.

Aurela, M., Tuovinen, J. P., & Laurila, T. (2001). Net CO_2 exchange of a subarctic mountain birch ecosystem. *Theoretical and Applied Climatology*, *70*(1-4), 135–148. https://doi.org/10.1007/s007040170011

Barr, A. G., Richardson, A. D., Hollinger, D. Y., Papale, D., Arain, M. A., Black, T. A., et al. (2013). Use of change-point detection for friction-velocity threshold evaluation in eddy-covariance studies. *Agricultural and Forest Meteorology*, *171*, 31–45.

Brix, H., Sorrell, B. K., & Orr, B. T. (1992). Internal pressurization and convective gas-flow in some emergent fresh-water macrophytes. *Limnology and Oceanography*, *37*(7), 1420–1433. https://doi.org/10.4319/lo.1992.37.7.1420

Brown, M. G., Humphreys, E. R., Moore, T. R., Roulet, N. T., & Lafleur, P. M. (2014). Evidence for a nonmonotonic relationship between ecosystem-scale peatland methane emissions and water table depth. *Journal of Geophysical Research: Biogeosciences*, *119*, 826–835. https://doi.org/10.1002/2013JG002576

Bubier, J., Moore, T., Savage, K., & Crill, P. (2005). A comparison of methane flux in a boreal landscape between a dry and a wet year. *Global Biogeochemical Cycles*, *19*, GB1023. https://doi.org/10.1029/2004GB002351

Chanton, J. P., Bauer, J. E., Glaser, P. A., Siegel, D. I., Kelley, C. A., Tyler, S. C., et al. (1995). Radiocarbon evidence for the substrates supporting methane formation within northern Minnesota peatlands. *Geochimica et Cosmochimica Acta*, *59*(17), 3663–3668. https://doi.org/10.1016/0016-7037(95)00240-Z

Ciais, P., Sabine, C., Bala, G., Bopp, L., Brovkin, V., Canadell, J., et al. (2013). Carbon and other biogeochemical cycles. In T. F. Stocker, et al. (Eds.), *Climate change 2013: The physical science basis. Contribution of working group I to the fifth assessment report of the Intergovernmental Panel on Climate Change* (pp. 465–570). Cambridge, UK and New York: Cambridge University Press.

Couwenberg, J., & Fritz, C. (2012). Towards developing IPCC methane 'emission factors' for peatlands (organic soils). *Mires and Peat*, *10*, 1–17.

Drebs, A., Nordlund, A., Karlsson, P., Helminen, J., & Rissanen, P. (2002). Climatological statistics of Finland 1971–2000, Finnish meteorological institute, Helsinki, 99 ISBN 951–697–568-2.

Dunfield, P., Dumont, R., & Moore, T. R. (1993). Methane production and consumption in temperate and subarctic peat soils, response to temperature and pH. *Soil Biology and Biochemistry*, *25*(3), 321–326. https://doi.org/10.1016/0038-0717(93)90130-4

Foken, T., & Wichura, B. (1996). Tools for quality assessment of surface-based flux measurements. *Agricultural and Forest Meteorology*, *78*(1-2), 83–105. https://doi.org/10.1016/0168-1923(95)02248-1

Fortuniak, K., Pawlak, W., Bednorz, L., Grygoruk, M., Siedlecki, M., & Zielinski, M. (2017). Methane and carbon dioxide fluxes of a temperate mire in Central Europe. *Agricultural and Forest Meteorology*, *232*, 306–318. https://doi.org/10.1016/j.agrformet.2016.08.023

Guenther, A. B., Jiang, X., Heald, C. L., Sakulyanontvittaya, T., Duhl, T., Emmons, L. K., & Wang, X. (2012). The model of emissions of gases and aerosols from nature version 2.1 (MEGAN2.1): An extended and updated framework for modeling biogenic emissions. *Geoscientific Model Development*, *5*(6), 1471–1492. https://doi.org/10.5194/gmd-5-1471-2012

Hargreaves, K. J., Fowler, D., Pitcairn, C. E. R., & Aurela, M. (2001). Annual methane emission from Finnish mires estimated from eddy covariance campaign measurements. *Theoretical and Applied Climatology*, *70*(1-4), 203–213. https://doi.org/10.1007/s007040170015

Hari, P., & Kulmala, M. (2005). Station for measuring ecosystem-atmosphere relations (SMEAR II). *Boreal Environment Research*, *10*, 315–322.

Hommeltenberg, J., Mauder, M., Drösler, M., Heidbach, K., Werle, P., & Schmid, H. P. (2014). Ecosystem scale methane fluxes in a natural temperate bog-pine forest in southern Germany. *Agricultural and Forest Meteorology*, *198–199*, 273–284.

Hui, D., Luo, Y., & Katul, G. (2003). Partitioning interannual variability in net ecosystem exchange between climatic variability and functional change. *Tree Physiology*, *23*(7), 433–442. https://doi.org/10.1093/treephys/23.7.433

IPCC (2013). Summary for Policymakers. In T. F. Stocker, et al. (Eds.), *Climate change 2013: The physical science basis. Contribution of working group I to the fifth assessment report of the Intergovernmental Panel on Climate Change* (pp. 3–29). Cambridge, UK and New York: Cambridge University Press.

Jackowicz-Korczyński, M., Christensen, T. R., Bäckstrand, K., Crill, P., Friborg, T., Mastepanov, M., & Ström, L. (2010). Annual cycle of methane emission from a subarctic peatland. *Journal of Geophysical Research*, *115*, G02009. https://doi.org/10.1029/2008JG000913

Joabsson, A., & Christensen, T. R. (2001). Methane emissions from wetlands and their relationship with vascular plants. *Global Change Biology*, *7*(8), 919–932. https://doi.org/10.1046/j.1354-1013.2001.00044.x

Joabsson, A., Christensen, T. R., & Wallén, B. (1999). Vascular plant controls on methane emissions from northern peatforming wetlands. *TREE*, *14*(10), 385–388.

Juottonen, H., Tuittila, E.-S., Juutinen, S., Fritze, H., & Yrjälä, K. (2008). Seasonality of rDNA- and rRNA-derived archaeal communities and methanogenic potential in a boreal mire. *The ISME Journal*, *2*(11), 1157–1168. https://doi.org/10.1038/ismej.2008.66

Kim, J., Verma, S. B., & Billesbach, D. P. (1998). Seasonal variation in methane emission from a temperate Phragmites-dominated marsh: Effect of growth stage and plant mediated transport. *Global Change Biology*, *5*, 433–440.

Kim, J., Verma, S. B., Billesbach, D. P., & Clement, R. J. (1998). Diel variation in methane emission from a midlatitude prairie wetland: Significance of convective throughflow in Phragmites australis. *Journal of Geophysical Research*, *103*(D21), 28,029–28,039. https://doi.org/10.1029/98JD02441

King, J. Y., & Reeburgh, W. S. (2002). A pulse-labeling experiment to determine the contribution of recent plant photosynthates to net methane emission in arctic wet sedge tundra. *Soil Biology and Biochemistry*, *34*(2), 173–180. https://doi.org/10.1016/S0038-0717(01)00164-X

King, J. Y., Reeburgh, W. S., Thieler, K. K., Kling, G. W., Loya, W. M., Johnson, L. C., & Nadelhoffer, K. J. (2002). Pulse-labeling studies of carbon cycling in Arctic tundra ecosystems: The contribution of photosynthates to methane emission. *Global Biogeochemical Cycles*, *16*(4), 1062. https://doi.org/10.1029/2001GB001456

Knox, S. H., Matthes, J. H., Sturtevant, C., Oikawa, P. Y., Verfaillie, J., & Baldocchi, D. (2016). Biophysical controls on interannual variability in ecosystem-scale CO_2 and CH_4 exchange in a California rice paddy. *Journal of Geophysical Research: Biogeosciences*, *121*, 978–1001. https://doi.org/10.1002/2015JG003247

Kowalska, N., Chojnicki, B. H., Rinne, J., Haapanala, S., Siedlecki, P., Urbaniak, M., et al. (2013). Measurements of methane emission from a temperate wetland by the eddy covariance method. *International Agrophysics*, *27*, 283–290.

Laine, A., Bubier, J., Riutta, T., Nilsson, M., Moore, T., Vasander, H., & Tuittila, E.-S. (2012). Abundance and composition of plant biomass as potential controls for mire NEE. *Botany*, *90*(1), 63–74. https://doi.org/10.1139/b11-068

Lamers, L. P. M., Vile, M. A., Grootjans, A. P., Acreman, M. C., van Diggelen, R., Evans, M. G., et al. (2015). Ecological restoration of rich fens in Europe and North America: from trial and error to an evidence-based approach. *Biological Reviews*, *90*, 182–203. https://doi.org/10.1111/brv.12102

Lees, K. J., Quaife, T., Artz, R. R. E., Khomik, M., & Clark, J. M. (2018). Potential for using remote sensing to estimate carbon fluxes across northern peatlands—A review. *Science of the Total Environment*, *615*, 857–874.

Levy, P. E., & Gray, A. (2015). Greenhouse gas balance of a semi-natural peatbog in northern Scotland. *Environmental Research Letters*, *10*, 094019.

Li, T., Raivonen, M., Alekseychik, P., Aurela, M., Lohila, A., Zheng, X., et al. (2016). Importance of vegetation classes in modeling CH_4 emissions from boreal and subarctic wetlands in Finland. *Science of the Total Environment*, *572*, 1111–1122. https://doi.org/10.1016/j.scitotenv.2016.08.020

Lloyd, J., & Taylor, J. A. (1994). On the temperature-dependence of soil respiration. *Functional Ecology*, *8*(3), 315–323. https://doi.org/10.2307/2389824

Mammarella, I., Launiainen, S., Gronholm, T., Keronen, P., Pumpanen, J., Rannik, Ü., & Vesala, T. (2009). Relative humidity effect on the high frequency attenuation of water vapour flux measured by a closed-path eddy covariance system. *Journal of Atmospheric and Oceanic Technology*, *26*(9), 1856–1866. https://doi.org/10.1175/2009JTECHA1179.1

Mammarella, I., Peltola, O., Nordbo, A., Järvi, L., & Rannik, Ü. (2016). Quantifying the uncertainty of eddy covariance fluxes due to the use of different software packages and combinations of processing steps in two contrasting ecosystems. *Atmospheric Measurement Techniques*, *9*(10), 4915–4933. https://doi.org/10.5194/amt-9-4915-2016

Marushchak, M. E., Friborg, T., Biasi, C., Herbst, M., Johansson, T., Kiepe, I., et al. (2016). Methane dynamics in the subarctic tundra: Combining stable isotope analyses, plot- and ecosystem-scale flux measurements. *Biogeosciences*, *13*(2), 597–608. https://doi.org/10.5194/bg-13-597-2016

Mathijssen, P., Väliranta, M., Korrensalo, A., Alekseychik, P., Vesala, T., Rinne, J., & Tuittila, E.-S. (2016). Reconstruction of Holocene carbon dynamics in a large boreal peatland complex, southern Finland. *Quaternary Science Reviews*, *142*, 1–15.

Mathijssen, P. J. H., Kähkölä, N., Tuovinen, J.-P., Lohila, A., Minkkinen, K., Laurila, T., & Väliranta, M. (2017). Lateral expansion and carbon exchange of a boreal peatland in Finland resulting in seven thousand years of positive radiative forcing. *Journal of Geophysical Research: Biogeosciences*, *122*, 562–577. https://doi.org/10.1002/2016JG003749

McVeigh, P., Sottocornola, M., Foley, N., Leahy, P., & Kiely, G. (2014). Meteorological and functional response partitioning to explain interannual variability of CO2 exchange at an Irish Atlantic blanket bog. *Agricultural and Forest Meteorology*, *194*, 8–19. https://doi.org/10.1016/j.agrformet.2014.01.017

Mikhaylov, O. A., Miglovets, M. N., & Zagirova, S. V. (2015). Vertical methane fluxes in mesooligotrophic boreal peatland in European Northeast Russia. *Contemporary Problems of Ecology*, *8*(3), 368–375. https://doi.org/10.1134/S1995425515030099

Nadeau, D. F., Rousseau, A. N., Coursolle, C., Margolis, H. A., & Parlange, M. B. (2013). Summer methane fluxes from a boreal bog in northern Quebec, Canada, using eddy covariance measurements. *Atmospheric Environment*, *81*, 464–474. https://doi.org/10.1016/j.atmosenv.2013.09.044

Oikawa, P. Y., Jenerette, G. D., Knox, S. H., Sturtevant, C., Verfaillie, J., Dronova, I., et al. (2017). Evaluation of a hierarchy of models reveals importance of substrate limitation for predicting carbon dioxide and methane exchange in restored wetlands. *Journal of Geophysical Research: Biogeosciences*, *122*, 145–167. https://doi.org/10.1002/2016JG003438

Olson, D. M., Griffis, T. J., Noormets, A., Kolka, R., & Chen, J. (2013). Interannual, seasonal, and retrospective analysis of the methane and carbon dioxide budgets of a temperate peatland. *Journal of Geophysical Research: Biogeosciences*, *118*, 226–238. https://doi.org/10.1002/jgrg.20031

Peltola, O., Hensen, A., Helfter, C., Belelli Marchesini, L., Bosveld, F. C., van den Bulk, W. C. M., et al. (2014). Evaluating the performance of commonly used gas analysers for methane eddy covariance flux measurements: The InGOS inter-comparison field experiment. *Biogeosciences*, *11*(12), 3163–3186. https://doi.org/10.5194/bg-11-3163-2014

Peltola, O., Mammarella, I., Haapanala, S., Burba, G., & Vesala, T. (2013). Field intercomparison of four methane gas analyzers suitable for eddy covariance flux measurements. *Biogeosciences*, *10*(6), 3749–3765. https://doi.org/10.5194/bg-10-3749-2013

Petrescu, A. M. R., Lohila, A., Tuovinen, J.-P., Baldocchi, D., Desai, A. R., Roulet, N. T., et al. (2015). The uncertain climate footprint of wetlands under human pressure. *Proceedings of the National Academy of Sciences*, *112*(15), 4594–4599. https://doi.org/10.1073/pnas.1416267112

Raivonen, M., Smolander, S., Backman, L., Susiluoto, J., Aalto, T., Markkanen, T., et al. (2017). HIMMELI v1.0: HelsinkI Model of MEthane buiLd-up and emIssion for peatlands. *Geoscientific Model Development*, *10*(12), 4665–4691. https://doi.org/10.5194/gmd-10-4665-2017

Rinne, J., Aurela, M., & Manninen, T. (2009). A simple method to determine the timing of snow melt by remote sensing with application to the CO_2 balances of northern mire and heath ecosystems. *Remote Sensing*, *1*(4), 1097–1107. https://doi.org/10.3390/rs1041097

Rinne, J., Riutta, T., Pihlatie, M., Aurela, M., Haapanala, S., Tuovinen, J.-P., et al. (2007). Annual cycle of methane emission from a boreal fen measured by the eddy covariance technique. *Tellus Series B*, *59*(3), 449–457. https://doi.org/10.1111/j.1600-0889.2007.00261.x

Riutta, T., Laine, J., Aurela, M., Rinne, J., Vesala, T., Laurila, T., et al. (2007). Spatial variation in plant communities and their function regulates carbon gas dynamics in boreal fen ecosystem. *Tellus Series B*, *59*(5), 838–852. https://doi.org/10.1111/j.1600-0889.2007.00302.x

Roulet, N. T., Lafleur, P. M., Richard, P. J. H., Moore, T. R., Humpreys, E. R., & Bubier, J. (2007). Contemporary carbon balance and late Holocene carbon accumulation in a northern peatland. *Global Change Biology*, *13*(2), 397–411. https://doi.org/10.1111/j.1365-2486.2006.01292.x

Saarinen, T. (1996). Biomass and production of two vascular plants in a boreal mesotrophic fen. *Canadian Journal of Botany*, *74*(6), 934–938. https://doi.org/10.1139/b96-116

Ström, L., Ekberg, A., Mastepanov, M., & Christensen, T. R. (2003). The effect of vascular plants on carbon turnover and methane emissions from a tundra wetland. *Global Change Biology*, *9*(8), 1185–1192. https://doi.org/10.1046/j.1365-2486.2003.00655.x

Ström, L., Falk, J. M., Skov, K., Jackowicz-Korczynski, M., Mastepanov, M., Christensen, T. R., et al. (2015). Controls of spatial and temporal variability in CH_4 flux in a high arctic fen over three years. *Biogeochemistry*, *125*(1), 21–35. https://doi.org/10.1007/s10533-015-0109-0

Suni, T., Rinne, J., Reissell, A., Altimir, N., Keronen, P., Rannik, Ü., et al. (2003). Long-term measurements of surface fluxes above a Scots pine forest in Hyytiälä, southern Finland, 1996–2001. *Boreal Environment Research*, *8*, 287–301.

Teklemariam, T. A., LaFleur, P. M., Moore, T. R., Roulet, N. T., & Humphreys, E. R. (2010). The direct and indirect effects of inter-annual meteorological variability on ecosystem carbon dioxide exchange at a temperate ombrotrophic bog. *Agricultural and Forest Meteorology*, *150*(11), 1402–1411. https://doi.org/10.1016/j.agrformet.2010.07.002

Tian, H., Xu, X., Liu, M., Ren, W., Zhang, C., Chen, G., & Lu, C. (2010). Spatial and temporal patterns of CH_4 and N_2O fluxes in terrestrial ecosystems of North America during 1979–2008: Application of a global biogeochemistry model. *Biogeosciences*, *7*(9), 2673–2694. https://doi.org/10.5194/bg-7-2673-2010

Turetsky, M. R., Kotowska, A., Bubier, J., Dise, N. B., Crill, P., Hornibrook, E., et al. (2014). A synthesis of methane emissions from 71 northern, temperate, and subtropical wetlands. *Global Change Biology*, *20*(7), 2183–2197. https://doi.org/10.1111/gcb.12580

Tyndall, J. (1862). On the absorption and radiation of heat by gaseous matter—Second memoir. *Philosophical Transactions. Royal Society of London*, *1862*(152), 59–98.

van den Berg, M., Ingwersen, J., Lamers, M., & Streck, T. (2016). The role of Phragmites in the CH4 and CO2 fluxes in a minerotrophic peatland in Southwest Germany. *Biogeosciences*, *13*(21), 6107–6119. https://doi.org/10.5194/bg-13-6107-2016

Volta, D. A. (1777). Lettere del Signor don Alessandro Volta Sull Aria Inflammabile Nativa delle Paludi [Letters of Signor don Alessandro Volta on the flammable native air of the marshes], Giuseppe Marelli, Milan, Italy.

Walter, B., & Heimann, M. (2000). A process-based climate-sensitive model to derive methane emissions from natural wetlands: Application to five wetland sites, sensitivity to model parameters, and climate. *Global Biogeochemical Cycles*, *14*(3), 745–765. https://doi.org/10.1029/1999GB001204

Wang, H., Richardson, C. J., & Ho, M. (2015). Dual controls on carbon loss during drought in peatlands. *Nature Climate Change*, *5*(6), 584–587. https://doi.org/10.1038/nclimate2643

Wania, R., Ross, I., & Prentice, I. C. (2010). Implementation and evaluation of a new methane model within a dynamic global vegetation model: LPJ-WHyMe v.1.3.1. *Geoscientific Model Development*, *3*(2), 565–584. https://doi.org/10.5194/gmd-3-565-2010

Watts, J. D., Kimball, J. S., Parmentier, F.-J. W., Sachs, T., Rinne, J., Zona, D., et al. (2013). A satellite data driven biophysical modeling approach for estimating northern peatland and tundra CO_2 and CH_4 fluxes. *Biogeosciences*, *11*(7), 1961–1980. https://doi.org/10.5194/bg-11-1961-2014

Webb, E. K., Pearman, G. I., & Leuning, R. (1980). Correction of flux measurements for density effects due to heat and water vapour transport. *Quarterly Journal of the Royal Meteorological Society*, *106*(447), 85–100. https://doi.org/10.1002/qj.49710644707

Whiting, G. J., & Chanton, J. P. (1992). Plant-dependent CH_4 emission in a subarctic Canadian fen. *Global Biogeochemical Cycles*, *6*(3), 225–231. https://doi.org/10.1029/92GB00710

Whiting, G. J., & Chanton, J. P. (1993). Primary production control of methane emission from wetlands. *Nature*, *364*(6440), 794–795. https://doi.org/10.1038/364794a0

Whiting, G. J., Chanton, J. P., Bartlet, D. S., & Happell, J. D. (1991). Relationships between CH_4 emission, biomass, and CO_2 exchange in a subtropical grassland. *Journal of Geophysical Research*, *96*(D7), 13067–13,071. https://doi.org/10.1029/91JD01248

Wille, C., Kutzbach, L., Sachs, T., Wagner, D., & Pfeiffer, E.-M. (2008). Methane emission from Siberian arctic polygonal tundra: Eddy covariance measurements and modeling. *Global Change Biology*, *14*(6), 1395–1408. https://doi.org/10.1111/j.1365-2486.2008.01586.x

Wilson, D., Alm, J., Riutta, T., Laine, J., Byrne, K. A., Farrell, E. P., & Tuittila, E.-S. (2007). A high resolution green area index for modelling the seasonal dynamics of CO_2 exchange in vascular plant peatland communities. *Plant Ecology*, *190*(1), 37–51. https://doi.org/10.1007/s11258-006-9189-1

Zhuang, Q., Melillo, J. M., Kicklighter, D. W., Prinn, R. G., McGuire, A. D., Steudler, P. A., et al. (2004). Methane fluxes between terrestrial ecosystems and the atmosphere at northern high latitudes during the past century: A retrospective analysis with a process-based biogeochemistry model. *Global Biogeochemical Cycles*, *18*, GB3010. https://doi.org/10.1029/2004GB002239